Accepted Manuscript

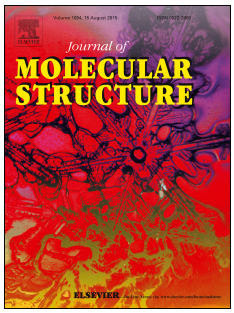

Novel bioactive azo-azomethine based Cu (II), Co (II) and Ni(II) complexes, structural determination and biological activity

N. Venugopal, G. Krishnamurthy, H.S. Bhojyanaik, M. Giridhar

PII: S0022-2860(19)30417-X

DOI: https://doi.org/10.1016/j.molstruc.2019.04.022

Reference: MOLSTR 26394

To appear in: *Journal of Molecular Structure*

Received Date: 18 January 2019

Revised Date: 8 March 2019

Accepted Date: 4 April 2019

Please cite this article as: N. Venugopal, G. Krishnamurthy, H.S. Bhojyanaik, M. Giridhar, Novel bioactive azo-azomethine based Cu (II), Co (II) and Ni(II) complexes, structural determination and biological activity, *Journal of Molecular Structure* (2019), doi: https://doi.org/10.1016/j.molstruc.2019.04.022.

"Novel bioactive azo-azomethine based Cu (II), Co (II) and Ni(II) complexes, structural determination and biological activity"

Venugopal N [a], Krishnamurthy G [a], Bhojyanaik H. S. [b*] Giridhar M [c].*

[a]*Department of chemistry, Sahyadri Science College, Kuvempu University, Shivamogga-577201, Karnataka, India.*

[b]*Department of Industrial chemistry, Kuvempu University, Jnana Sahyadri, Shankaraghatta, Shivamogga-577451, Karnataka, India.*

[c]*Government First Grade College (GFGCH), Hassan-573201, Karnataka, India.*

[*]**Email: gkmnaiksahydri@gmail.com**

Abstract

A novel bioactive azo-azomithine tridentate ligand N'-[(E)-{2-hydroxy-3-methoxy-5-[(E)phenyldiazenyl]phenyl}methylidene]pyridine-3 carbohydrazide **(HL)** and its Cu(II), Co(II) and Ni(II) complexes were synthesized and their structure determined by elemental analysis, spectroscopic studies (FTIR, ^{1}H NMR, ^{13}C NMR, LC-MS, UV-vis, ESR, and powder XRD) and magnetic susceptibility measurements. The molar conductivity measurement proved that all the complexes are non-electrolytic in nature. On the basis of physicochemical and spectroscopic data, the octahedral geometry is assigned for all the metal complexes. The thermal decomposition curve indicated the existence of lattice water molecule. The binding studies of all the synthesized complexes against CT-DNA suggest that the intercalation binding mode. A DNA nuclease activity exhibited that all complexes cleaved pBR322 DNA in an efficient manner. Consequently, the cytotoxic activity of the compounds was screened against A-549 (lung carcinoma), MDA-MB 231 (breast carcinoma) and normal HEK293 (human embryonic kidney cells) cell lines using MTT assay.

Keywords: Metal chelates; P–XRD; TGA-DTG; DNA interaction; Cytotoxicity.

Introduction

Over the last few decades, remarkable step have been taken in designing of transition metal chelates of azomethines, which are utilized in an extensive range of biological and clinical applications along with remedial drug against cancer cells [**1**]. Cancer is becoming a leading cause of premature lethal death in most of the developed as well as developing countries [**2**]. To examine the clinical application of transition metal based tumour drugs one important point is minimization the undesirable side effect of the drug [**3**]. *Cis*platin, carboplatin, and oxaliplatin (with many severe side effects) were major tumour drugs for some decades thus developing novel metal–based complexes with less-toxicity and target specific in an active area of research[**4**].The deoxyribonucleic acid (DNA) plays an essential role in the replication of cells and storage of genetic information**[5].** DNA is the primary intercellular target for many tumour drugs in clinical use and important to understand the binding of metal ion to DNA through both covalent and non-covalent interactions **[6]**. Three known non-covalent binding modes of small molecule to DNA are intercalative binding, groove binding and external electrostatic binding **[7]**. Among these, intercalative binding mode is most important and coherent to the anticancer activity the metal ion [**8**].

The pyridine-anchored hydrazone moiety have recognised significant interest due to the presence of donar atom like nitrogen and oxygen has achieved dazzling coordination capacity and diverse pharmacological activities **[9-11]**. In addition, the phenolic aldehyde compounds like vanillin are well known and perform a class of molecule which show a comprehensive biological property **[12, 13]**. An added privilege of using 2-hydroxy-3-methoxy-5-[(*Z*)-phenyldiazenyl] benzaldehyde over vanillin is the position of hydroxyl group, this group is present at ortho position can readily deprotonate and coordinate with metal centre [**14**]. Hence, an imense number of Cu (II), Co (II) and Ni (II) complexes of azo-dye Schiff bases have been extensively studied due to their diverse antifungal, antibacterial, anti-tuberculosis, anticonvulsant and anticancer activities. Thus, the design of new chemotherapeutic drug is now engaging the consideration of medicinal chemists which reduce the toxicity [**15-17**]. Furthermore, the interaction of compounds with double helix DNA has been widely studied, due to the site of specific binding and many significant applications in cancer therapy. These coordination compounds were also important in developing probes for nucleic acid structures and cancer drugs [**18, 19**].

This paper describes, the synthesis of novel bioactive Cu (II), Co (II) and Ni (II) complexes of the azo linked Schiff base N'-[(E)-{2-hydroxy-3-methoxy-5-[(E)phenyldiazenyl] phenyl}methylidene]pyridine-3 carbohydrazide (**HL**) and characterized by various analytical

and spectroscopic techniques. The electronic and thermal techniques were used to deduce the geometry of the metal complexes. DNA-binding behaviour of metal complex was investigated via electronic absorption spectroscopy. The DNA cleavage activity of metal complexes performed using gel electrophoresis technique using supercoiled pBR322 DNA. Additionally, *in-vitro* anticancer activity of synthesized complexes was assessed by MTT assays, against cancer cell lines A-549, MDA-MB 231 and normal HEK293 cells.

2. Experimental

2.1. Reagents and Physical Measurements

All the reagents needed for the present work were commercially available, analytical grade and obtained from Sigma Aldrich, Merck and Hi Media Ltd., utilized without further purification. Microanalytical data (Carbon, Hydrogen and Nitrogen) was carried out on Vario EL.CHNOS elemental analyser. The electronic spectra of the compounds were recorded on shimadzu model 1650 UV- visible double beam spectrometer in the range of 200–800 nm in DMF solution (10^{-3}M). FTIR spectra recorded using KBr discs on a Bruker alpha-T FTIR Spectrophotometer in the range of 4000-400cm^{-1}. ^{1}H and ^{13}C NMR spectra were obtained using a Bruker DPX200 instrument (400 MHz) in DMSO-d_6 as a solvent consisting TMS as the internal reference compound. The mass spectral analysis was done on LC-MS: water AQUITY-2777C mass spectrometer. The conductivity measurement of the metal complexes was carried out in (10^{-3}M) DMF solution using an ELICO-CM82 conductivity bridge. The EPR spectrum of copper complex was recorded on JES - FA200 ESR spectrometer with solid state X-band at room temperature. The magnetic moment values of the complexes were calculated at room temperature on a Gouy balance model 7550 applying Hg [Co (NCS)$_4$] as a calibrant. Thermal analysis was recorded using SII Exstar TG/DTA 6300 instrument in the temperature range 30 to 800 ^{o}C with a heating rate of 10 ^{o}C min. The powder X- ray diffraction studies of the complexes were obtained on Bruker AXS D8 prior instrument.

2.2. Synthesis of of Azo Schiff base ligand (HL)

Azo-linked Schiff base ligand **(HL)** was prepared in two steps. In the first step, diazonium solution was prepared by dissolving (2mmol) of aniline in 20 mL of distilled water and (4mL) of concentrated hydrochloric acid. The solution was cooled to 0-5 ^{o}C in an ice bath and a cold aqueous solution of sodium nitrite (2 mmol) in 3mL of concentrated sulphuric acid was added dropwise with continuous stirring. The obtained diazonium salt solution was stirred and cooled to 0-5 ^{o}C in an ice bath for about 1h and then poured drop wise to the

chilled solution of 2-hydroxy-4 methoxybenzaldehyde (2mmol) in alkaline media. The resulting mixture was stirred for about 2 h at the same temperature and the pH was maintained around 7.0-8. Coupling to the o-vanillin has occurred in basic media at the para position.

In the second step, 1:1 condenstion reaction occured between (2 mmol) 2-hydroxy -3 methoxy -5-(phenyldiazenyl) benzaldehyde and (2 mmol) of isonicotine hydrazide which were dissolved in hot ethanolic solution in the presence of 2-3 drops of glacial acetic acid as a catalyst. The reaction mixture was refluxed and continuously stirred for about 3-4h. After cooling, the azo-azomethine a dye was collected by filtration, washed with ethanol and dried in vacuum desiccator over $CaCl_2$. The purity of the compounds was achieved by the recrystallization in ethanol and the schematic depiction of the synthesis of ligand displayed in **Scheme 1.**

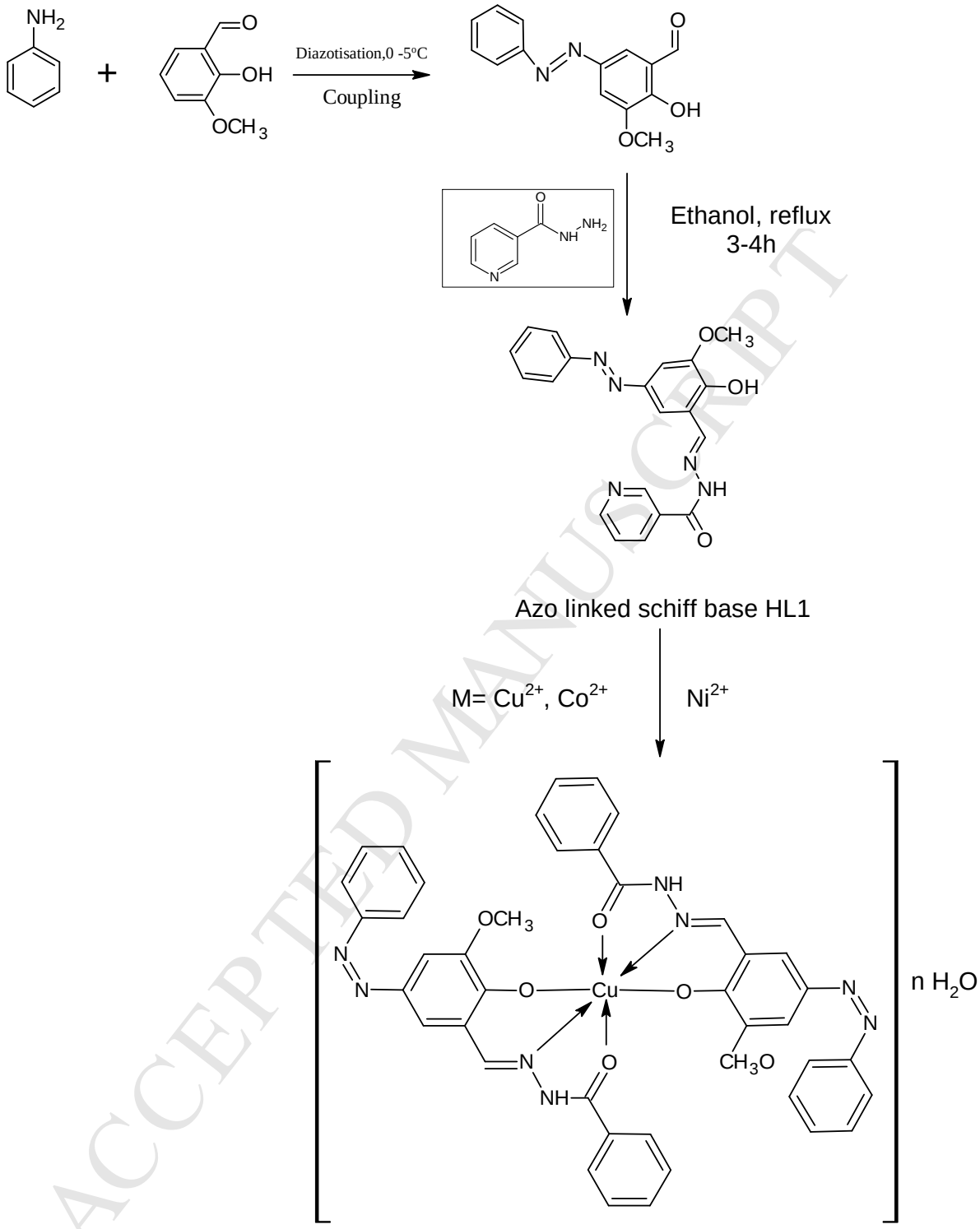

Where M=Cu (II) n=3, Co (II) and Ni(II) n=2.

2.2.1 N'-[(E)-{2-hydroxy-3-methoxy-5-[(E)-phenyldiazenyl]phenyl}methylidene]pyridine-3 carbohydrazide (HL).

Yield: (77.0 %), Colour: orange, melting Point: 254–256°C. Anal. Calc. For [$C_{20}H_{17}N_5O_3$] C, 57.42; H, 3.76; N, 10.65. Found C, 57.44; H, 3.78; N, 10.62. IR data on KBr pellet ν(cm^{-1}) :3246 ν(–OH), 3058 ν(N–H), 1602 ν(CH=N),1661 ν(C=O), 1444 ν(–N=N–).^{1}H NMR (400 MHz, DMSO-d_6, δ ppm): 12.40 (s, 1H, OH), 11.38 (s, 1H, NH); 8.85 (s, 1H, N=CH), 8.84 (d, 2H, *J*=10 Hz, pyridine *α*-H), 8.00–7.53 (m, 9H, Ar-H), 3.97 (s, 3H, OCH_3). ^{13}CNMR (100 MHz, DMSO-d_6, δ ppm): 161.98, 152.4, 150.88, 149.36, 147.55, 131.38, 129.91, 122.71, 119.77, 118.70, 104.79, and 56.49. LC-MS: m/z 376 [M+1]. UV–Vis (λ_{max}, nm): 246, 410.

2. 3 Synthesis of Cu (II), Co (II) and Ni (II) complexes

To the hot ethanolic solution of azo-azomethine ligand (2mmol) and appropriate metal chlorides Cu(II), Co(II) and Ni(II) in ethanol (1mmol) was added drop wise with constant stirring. The resulting suspension was refluxed on a steam bath for about 3-4 h. On cooling, the colored solid product was filtered and washed thoroughly with hot water and ethanol and dried in a vacuum over anhydrous $CaCl_2$.

2.4 Biological studies

2.4.1 DNA interaction studies

The binding interaction between the metal ions and CT-DNA was investigated using UV-vis spectroscopy. The required amount of DNA solution was prepared by dissolving in buffer medium (50 mM NaCl, 5 mM *Tris*-HCl and pH 7.2) UV absorbance value at 260 and 280 nm gave a ratio of about 1.8–1.9, revealing that DNA is clear from protein contamination. The concentration of CT-DNA per nucleotide was determined from its absorbance by employing a molar extinction coefficient value of 260 nm (Ɛ = 6600 M^{-1} cm^{-1}) [**20**]. The metal complexes were dissolved in DMSO solvent because of low solubility in buffer solution. Absorption titration studies were carried with a fixed concentration of the complexes (20 mM), by varying the concentration of DNA (20-350 mM). An equal volume of CT-DNA was added to both complex solution and reference solution in order to remove the absorbance of CT-DNA itself. The intrinsic binding constant (K_b) values of the complexes with DNA were measured by the following equation.

$$\mathbf{[DNA]/(Ɛ_a - Ɛ_f) = [DNA]/(Ɛ_b - Ɛ_f) + 1/K_b\,(Ɛ_b - Ɛ_f)} \qquad \longrightarrow 1$$

Where [DNA] is the concentration of CT-DNA in base pairs, $Ɛ_a$ is apparent coefficient of A_{obsd}/[complex], $Ɛ_f$ and $Ɛ_b$ correspond to the extinction coefficients of the free

and fully bound forms of the complex, respectively. A plot of [DNA] / ($\varepsilon_a - \varepsilon_f$) versus [DNA] gave a slope of 1/($\varepsilon_b - \varepsilon_f$) and Y-intercept equal to 1/ $K_b(\varepsilon_b - \varepsilon_f)$, K_b is the ratio of slope to intercept.

2.4.2 DNA cleavage activity

The interaction of newly synthesized metal complexes with DNA was carried out by using gel-electrophoretic technique [**21**]. The experiment involves pBR322 DNA (2 μL, 2 μg), 100 μg metal complexes, 50 mM *Tris*-HCl buffer, 50 mM NaCl were mixed and pH 7.2 was mantained. The contents were allowed to proceed with incubation for 2 h at 37 °C. After incubation, 5 μL of loading buffer (bromophenol blue 0.25%, Xylene cyanol 0.25% and glycerol 30%) and samples were poured into the well along with standard DNA marker on 1% agarose gel for 1 h at 60 mV. The gel was further blemished with 1μg cm^{-3} ethidium bromide solution for 10 min. The bands were observed under ultraviolet light and picture was taken.

2.4.3 Cell culture

The cell lines A-549, MDA-MB 231 and normal HEK293 were procured from NCCS Pune. The cells were cultivated in monolayer in RPMI 1640 medium, added with 10% fetal bovine serum (FBS) 2 mM L-glutamine, and 1% penicillin. Cells were preserved in 5% CO_2 at 37 °C in 95% relative humidity and clear from mycoplasma contamination.

2.4.4 Cell viability assay

The *in vitro*-anticancer activity was performed using MTT assay. Cells were grown in 96 well tissue culture plates at a concentration of (1×10^4 cells/well) and overnight incubation at 37 °C in 5% CO_2 under a moistened air atmosphere to permit the growth and attachment. Then the cells were treated with various concentration of complexes dissolved in DMSO (1-100μg mL^{-1}) and incubated for 24h. After incubation, the culture is detached and 20 μl MTT solution was added to each well. The plates were further incubated in darkness at the temperature of 37°C for about 4 h in CO_2 atmosphere. The following media is discarded in order to solubilise the purple colored formazan product by adding 200μl of DMSO is poured to each well. The absorbance of the wells was measured using the ELISA reader at 570 nm [**22, 23**]. The % of cell inhibition expressed as

Inhibition (%) = 1 – 100 × (OD toxicant) / (OD –ve control).

IC_{50} values were evaluated using the nonlinear regression program from origin.

3. Result and Discussion

The newly synthesized azo-azomethine dye ligand (**HL**) and their metal complexes were found to be tinted solid, stable at room temperature, soluble in DMF and DMSO. The observed molar conductivity measurement proved that all the metal complexes are non-electrolytic in nature [**24**]. Melting points of the prepared complexes were found to be above 300 ^{o} C. From the analytical data, it is evident that 1:2 stoichiometric ratio of metal to ligand with general a formula $[M(L)_2]\ nH_2O$ for all the complexes. The elemental analysis data are in good accordance with the calculated values. Physical measurement and analytical data of the ligands and its metal complexes are depicted in **Table 1**.

<Insert Table 1>

3. 1 ^{1}H and ^{13}C NMR spectrum of ligand

The ^{1}H and ^{13}C NMR spectrum of the ligand (**HL**) (Fig. S1 and S2) was obtained in DMSO-d_6 at room temperature using TMS as an internal standard. The ^{1}H NMR spectrum of azo azo-mithine ligand displayed a signal at 12.40 ppm as singlet which is attributed to the hydroxyl group attached to vanillin ring. The NH proton attached to isonicotine hydrazide next to carbonyl group appeared as a singlet at 11.38 ppm. The signal appeared at 8.85 ppm as a singlet is ascribed to azomethine proton (–CH=N). Another doublet found at 8.84 ppm is considered as the signal of the two protons at the alpha position of pyridine. Other aromatic ring protons of the ligands were resonated as multiplets in the range 8.00–7.53 ppm. Another singlet appeared at 3.97 ppm corresponds to the methoxy proton attached to vanillin ring [**25-27**].

The ^{13}C NMR spectrum of the ligand showed a signal at δ 161.98 ppm due to carbon of carbonyl group. The peak at δ 152.4 ppm due to azomethine carbon. All the other aromatic carbon shifts were observed in the range of δ 104.7–150.8 ppm. The peak at δ 55.9 ppm is assigned to the carbon atom of methoxy group [**28**].

3. 2 Mass spectra

The mass spectra of the ligand and its metal complexes were recorded and obtained molecular ion peak confirms the proposed formulae. The mass spectrum of ligand (**HL)** shows (Fig. S3) a well defined molecular ion peak at m/z 377 which was coincident with

(M+1) proposed molecular formula weight of azo-azomethine ligand. The molecular ion peaks of the Cu(II), Co(II) and Ni(II) complexes were appeared at m/z of 848, 844 and 845 respectively, which are equivalent to the stoichiometric ratio of 1:2 (M:L) type. Further, the observed molecular mass in all the spectra of the prepared complexes are in consistency with their proposed molecular structures.

3.3. Infrared spectra

The Infrared spectra of ligand **(HL)** and their metal complexes were recorded as KBr pellets in the region 4000-400 cm^{-1} and the data indicate the binding modes of the ligand to metal ion as presented in **Table 2**. The ligand exhibited a sharp band at 1602 cm^{-1} is due to υ (C=N) stretching vibration. On complexation, this band shifted to a lower frequency in the range of 1545-1563 cm^{-1} by about 29-55cm^{-1}in all the complexes indicating the involvement of azomethine nitrogen atom in coordination with the metal ion [**29**]. The appearance of a strong absorption band at 1661 cm^{-1} in spectrum of ligand assigned to υ(C=O) vibration which is shifted to lower frequency by 54 to 63 cm^{-1} in complexes and observed in the range 1598-1607cm^{-1} respectively, suggesting that the involvement of carbonyl group in bonding with the metal ions [**30**]. The characteristic broad band at 3058 cm^{-1} in the uncoordinated ligand is assignable to υ(NH) stretching vibration, which remains more or less at the same position in the spectra of all the complexes, indicating their non-involvement of amide group on complexation [**31**]. The IR spectra of free ligand showed a absorption band at 3225 cm^{-1} is ascribed to υ(-OH) group which disappeared in their spectra of metal complexes, indicating that the complex formation has taken place by deprotonation of phenolic oxygen atom.[**32**] The appearance of medium intensity band at 1444 cm^{-1} in the free ligand was assigned to stretching frequency of azo group (–N=N–). In all the complexes, this band lies at the same position confirming the non-participation of azo group in complex formation [**33**]. Furthermore, the existence of two new non-ligand bands in the region 495–460 cm^{-1} and 622– 555 cm^{-1} has been ascribed to M–N and M–O bands, respectively [**34**]. In conclusion, the IR data confirms a tridentate nature of the ligand.

<Insert Table 2>

3.4. Electronic spectral studies

The electronic absorption spectra of all the compounds were recorded using DMF solution in the range 200-800 nm at room temperature. The spectral data of the uncoordinated ligand exhibited two recognizable absorption bands. The absorption band appeared at 287 nm

(34,843cm^{-1}) may be ascribed to the $\pi \rightarrow \pi^*$ transition of the aromatic rings, while the other band appeared at 349 nm (28,653cm^{-1}) may be assigned to n$\rightarrow\pi^*$ electronic transition due to the azo-methine group respectively. Further, it is recognized that the absorptions bands were shifted to longer wavelength in all the metal complexes suggesting that ligands coordinate to metal ions [**35**].

Electronic spectrum of Cu(II) complexes exhibited two intra ligand charge transfer bands in the range of 24,875, 30,769 along with d–d transition band at 17,064 cm^{-1} due to the $^2E_g \rightarrow {}^2T_{2g}$ transition. The position of these bands suggests that the Cu(II) complex has a distorted octahedral geometry [**36**]. This is further favoured by its magnetic moment value of 1.82 B.M. The electronic spectrum of Co(II) complex exhibit three bands at 14,598, 16393 and 23,529cm^{-1} which are attributed to $^4T_{1g} \rightarrow {}^4T_{2g}(F)$, $^4T_{1g} \rightarrow {}^4A_{2g}(F)$ and $^4T_{1g} \rightarrow {}^4T_g(P)$ transition, respectively. The position of these bands and their magnetic moment value of 4.21 B.M, suggests that the Co(II) complex has a characteristic of octahedral geometry [**37**]. The electronic spectrum of Ni (II) complexes exhibit three bands at 16,103, 24,630 and 32,258 cm^{-1} attributed to $^1A_{1g} \rightarrow {}^1B_{1g}$, $^1A_{1g} \rightarrow 1A_{2g}$, and charge transfer transition. The positions of these bands and its magnetic moment value of 3.28 B. M, indicate an octahedral geometry [**38**].

3. 5 Electron spin resonance (ESR)

The X-band ESR spectrum of the Cu(II) complex of ligand **HL** was measured in the solid state at room temperature and is displayed in **Fig. 1.** The investigation of g value of copper complex provided the g tensor value $g_{\parallel}$=2.1438, $g_{\perp}$=2.0380 and G=4.04. It is known that if $g_{\parallel}$ value is greater than 2.3, then the M–L bond is virtually anionic character and the value is less than 2.3 is an indication of covalent nature [**39**]. In present case the observed $g_{\parallel}$ value of the copper complex is less than 2.3 indicating that appreciable covalency in metal–ligand bond. The trend in observed g values of the Cu(II) complex is $g_{\parallel}$ (2.1438) > $g_{\perp}$ (2.0380) > 2.0023, indicating that the unpaired electron in the ground state of Cu(II) is predominantly in d_{x2-y2} and the complex is axially symmetric. Thus, an octahedral structure is deduced for the complex [**40**]. G = ($g_{\parallel}$ -2) / ($g_{\perp}$-2) which determines the exchange interaction between the copper centres in the polycrystalline compound have been evaluated. According to Hathaway and Billing expression, if the G value is less than 4, the exchange interaction between the copper centers is noticed whereas if its value is greater than 4 the exchange interaction is negligible [**41**]. The calculated G value for the present Cu(II) complex was

4.042 indicating that there is an absence of exchange interaction between the copper ions. The observed g_{av} is 2.053. The ESR spectral parameters are given in Table 3.

<Insert Table 3>
<Insert Figure 1>

3.7. Thermal analysis

The thermal properties of Cu(II), Co(II) and Ni(II) complexes were carried out to understand the thermal stability and molecular structure. The tentative thermal decomposition of metal complex with respect to temperature and formation of the respective metal oxides are displayed in **Table 4.** The Thermal behaviour of the complexes were done from room temperature to 800 °C at a heating rate of 10 °C/min in a N_2 atmosphere is shown in **Fig. 2**. The thermogram of [Cu($C_{40}H_{38}N_{10}O_9$)] complex (**1a**) showed three decomposition stages, the first stage of decomposition occur in the temperature range 30-78°C is due to the elimination of three lattice water molecules with an approximate loss of 6.06% (calcd 6.23%). The second stage of decomposition occurs below the temperature 250 °C which corresponds to the loss of C_4O_2 molecules with a mass loss 9.18% (calcd 9.30%). The third stage of decomposition occurs within the temperature range 250-370 °C and corresponds to the loss of $C_{10}H_{10}N_2$ molecules with a mass loss 17.96% (calcd 18.26%). Further the complex underwent fourth stage of decomposition due to complete decomposition of organic portion $C_{24}H_{28}N_8O_3$ of complex in the temperature range 370-697°C with weight loss of 54.72% (calcd 55.02%). The weight of the residue corresponds to the one mole of cupric oxide and two moles of carbon.

The thermogram of [Co($C_{40}H_{36}N_{10}O_8$)] **(1b)** showed three decomposition stages, the first stage of decomposition occured within the temperature range at 26-75 °C is due to the loss of two water molecules with a weight loss of 4.26% (calcd 4.35%). The second stage of decomposition occurs within the temperature range 75-315 °C and corresponds to the loss of $C_{12}H_{10}N_2O_2$ molecules with a mass loss 24.29% (calcd 24.48%). Further third stage of decomposition occur in the temperature range 315-495 °C due to the loss of organic moiety of the complex $C_{28}H_{24}N_8O_3$ with the weight loss 55.86% (calcd 56.46%). The final weight of the residue corresponds to the one mole of cobalt oxide.

Similarly, the thermogram of [Ni($C_{40}H_{36}N_{10}O_8$)] **(1c)** showed four decomposition stages, in the temperature range 28-65 °C, 65-175 °C, 175-378 °C and 378-510 °C respectively. The

weight loss 4.25% (calcd 4.46%), % 15.56 (calcd 15.71%), 12.64% (calcd 13.03%) and 57.10% (calcd 58.29%) are tentatively ascribed to the removal of $2H_2O$, $C_8H_4O_2$, $C_4H_2N_2O_2$ and $C_{28}H_{28}N_8O_3$ fragments. Finally, one mole nickel oxide as residue was observed.

<Insert Table 4>
<Insert Figure 3>

3.8. Powder XRD studies

The powder X-ray diffraction patterns of the newly synthesized metal complexes were recorded because these complexes are soluble in polar organic solvents, like DMSO and DMF. Therefore single crystal could not be obtained. In order to understand the degree of crystallinity of the synthesized metal chelates, the X-ray diffractogram of Cu(II), Co(II) and Ni(II) complexes were obtained in the range of 10-80 (2θ) at a wavelength of 1.54 Å. All the metal complexes were displayed a certain amount of well defined sharp crystalline peaks proved inherent crystalline nature of complexes **Fig. 3**.

Powder X-ray diffraction pattern for Cu(II) complex showed 8 reflections in the range of 9-40 ° (2θ). The inter-planar spacing (d values) of the reflections were calculated using Bragg's equation $n\lambda = 2d\sin\theta$ (where λ=1.5406 Å). The observed and calculated inter-planar spacing (d) simultaneously, with relative intensities with respect to most intense peak are consistent and are depicted in **Table 5.** Further, the unit cell parameters were evaluated for cubic symmetry by all the important peaks, and $h^2 + k^2 + l^2$ values were ascertained. The observed inter-planer d-spacing values have been compared with the calculated ones and it was found to be in good agreement. The $h^2 + k^2 + l^2$ values for Cu(II) complex are 1, 2, 3, 4, 6, 10 and 15. It was noticed that the existence of forbidden number 15 suggests that the Cu(II) complex may reside to hexagonal or tetragonal systems. The calculated lattice parameter for Cu (II) complex is found to be $a = b = c = 8.05$.

Similar calculations were carried out for Co(II) and Ni(II) complexes and all the obtained major intense peaks have been indexed and observed values of inter-planar d-spacing have been compared with the calculated ones. The $h^2 + k^2 + l^2$ values for Co(II) complex are 1,1, 2, 2, 3, 4, 6, 7, 8, 10, 14 and for Ni(II) complex are 1, 1, 2, 3, 4, 6, 8, 10, 15. The presence of forbidden numbers like 7 for Co(II) complex and 15 for Ni (II) complex indicates both the complexes may belong to hexagonal or tetragonal systems. The lattice parameter for the Co(II) and Ni(II) complexes were found to be $a = b = c = 7.86$ and 8.108 respectively.

<Insert Table 5 >

<Insert Figure 3>

3.8. Scanning electron microscopy (SEM)

The surface morphology of the azo-azomethine ligand and its complexes were examined by scanning electron microscopy (SEM). **Fig. 4** illustrates the SEM photographs of the studied compounds. The broken rock like structure was observed in ligand **(HL)**.The ice block like structure with layered morphology has observed in Cu (II) complex. Particles are embede in cotton-like a filamentary matrix has observed in Co(II) complex and Ni(II) complex seemed as non uniform grain like structure, respectively. SEM images disclosed that the surface morphology of metal complexes vary from ligand and other because of the complexation and change of metal ion.

<Insert Figure 4>

4. Biological activities

4.1. DNA binding experiments

Electronic absorption spectroscopy is universally engaged technique to examine the strength and mode of binding of the metal complexes with DNA which generally involves the changes in absorbance and wavelength. The absorption spectra of Cu (II), Co (II) and Ni (II) complexes recorded in the absence and presence of CT-DNA are depicted in **Fig.5** The absorption titration were carried using a fixed metal complexes concentration to which increment of CT-DNA stock solutions was added in different ratio ranging from 25 mL to 350 mL. While calculating the absorption spectra of complexes, an equal amount of DNA was added to both the compound solution and the reference solution to eliminate the absorbance of DNA itself. The binding nature of metal ions to DNA was determined from the changes in absorbance spectrum of every complex upon supplement of CT-DNA. After the interaction of compounds with CT-DNA base pairs, the π^* orbital of the intercalated ligand on the complexes can couple with π orbitals of the DNA base pairs of DNA which leads to decrease in π-π^* transition energies. On the other hand, as the coupling π^* orbital are partially filled by electrons, decreases the transition probabilities resulting in hypochromism [**42**]. Upon gradually increasing the amount of CT-DNA to the complexes leads to considerable hypochromic effect without varying the absorption intensities. The hypochromicity, feature of intercalation is frequently assigned to the interaction between the planar aromatic

chromospheres of molecule and base pair of DNA [**43**]. These results revealed that the complex can bind to DNA *via* an intercalation mode of the double helix DNA. The percentage of hypochromism of the complexes were found to be 24 –37% with red shift of 1-4 nm.

In order to determine significantly the binding potency of these complexes, the intrinsic binding constant (K_b) of the metal complexes (**1a**–**1c**) with DNA was determined by equation (1). The K_b values are found to be $5.6 \times 10^5 M^{-1}$, $4.48 \times 10^5\ M^{-1}$ and $3.79 \times 10^5\ M^{-1}$, respectively, revealing greater binding tendency of complex **1a** as compared to **1b** and **1c**. From the above result it is clear that, the Cu (II) complex show strong binding affinity to DNA than Co (II) and Ni (II) complexes. The binding efficiency of metal chelates toward DNA depends on the coordination number and nature of metal atom in the complex.

<Insert Figure 5>

*4.2.**DNA cleavage studies***

The investigation on the cleaving affinity of metal complexes to DNA is very fascinating because it can furnish to understanding the toxicity mechanism of them and to develop novel artificial nuclease. The DNA cleavage study of the synthesized metal complexes was performed by agarose gel electrophoretic technique using pBR322 plasmid DNA as a substrate. When circular plasmid DNA is subjected to electrophoresis, the relatively fastest journey will be obtained for the supercoiled form (Form I). If one strand slashed, the supercoil will unwind to produce a slowest moving nicked form (Form II). If both strands are cleaved, a linear form (Form III) will be produced and migrates in between Form I and Form II [**44**]. The plasmid pBR322 plasmid DNA (100 ng) were mixed with a fixed concentration of metal complexes. **M** – is standard DNA molecular weight marker, Lane **1** applies to the untreated pBR322 plasmid DNA (control DNA) which was initially found to be mixture of mainly of super coiled form I and a small amount of singly-nicked form II [**45**] as shown in **Fig.6.** The plasmid DNA interaction with the complexes leads to one strands break of the DNA, and the circular form (II) is observed. Lane 2 **(1a)** has partially cleaved both the form I and form II DNA, lane 3 and 4 **(1b & 1c)** were effectively cleaved supercoiled DNA (form I) to nicked DNA (form II). Thus, the complexes show DNA nuclease activity in the absence of any external agent. Moreover, the quantity of helical unwinding caused by the complex bound to supercoiled offers proof for the intercalation mode of interaction between the compounds and DNA [**46**]. Thus, we can draw a conclusion that the newly synthesized metal

complexes under the present study are good inhibitor for the growth of the pathogenic microorganism by cleaving the plasmid DNA.

<Insert Figure 6>

4.3.In-vitro cytotoxic activity by MTT assay

The cytotoxic activity of the synthesized azo-azomithine ligand and its metal complexes on the proliferation of human lung cancer cells (A-549), breast cancer cells (MDA-MB 231) and normal embryonic kidney cells (HEK293) were examined by MTT assay. Cisplatin was taken as a reference drug and the cells were treated with various concentrations of metal complexes (1, 2, 5, 10, 25, 50 and 100 μg mL^{-1}) for 24 h. The dose dependent half-inhibitory effects of ligand and its complexes on cell viability of different human cancer cell lines showed in **Fig. 7-9**. From the figures, it is clear that on increment in the concentrations of compounds exhibited diminish in cell viability deducing enhanced cytotoxicity. The IC_{50} values obtained for the compounds against the screened cell lines are offered in **Table 5**, and were compared with cisplatin. All the complexes exhibited strong potent cytotoxicity against A-549 and MDMB-231 cancer cells, IC_{50} value ranged from 4.759-41.25 and 5.836–58.51 μg/ ml. While all the metal complexes are less toxic toward the normal cell as it evident from the higher IC_{50} value 25.17–79.52 μg/ml, respectively. Evidently, the azo-azomethine ligand exhibited less inhibition on the cancer cells, but the complexes showed good cytotoxic activities relative to cisplatin. The higher activity of metal complex may be due to the increase in their lipophibility on chelation. Moreover, the activity of the metal complex depends on the nature of central metal ion present in the metal complexes. In the present work, the **Cu (II)** complex showed good activity when compared to the remaining complexes against all the screened cell lines.

<Insert Table 6>

<Insert Figure 7, 8 and 9 >

3. Conclusion

The azo azo-methine ligand **HL** and their **Cu(II), Co(II)** and **Ni(II)** complexes were synthesized and structurally characterized by various analytical and spectroscopic techniques. The analytical data reveal that the metal complexes have 1:2 metal to ligand ratio. The molar conductance data indicate that the complexes are non-electrolytic in nature. The electronic spectra and magnetic moment measurement indicated that all the complexes having an

octahedral geometry. The synthesized metal complexes showed different surface morphological structure as appeared in SEM and powder XRD, TGA spectra of metal complexes showed the existence of lattice water molecule and gave good result in thermal stability. Moreover, the interaction of metal complexes with CT-DNA have been effectively investigated by electronic absorption spectroscopy, the result revealed that the metal complexes bind to CT-DNA through an intercalative mode. The DNA cleavage activity revealed that all the metal complexes effectively cleaved supercoiled pBR322 DNA without any external agent. Moreover, the *in-vitro* cytotoxicity of ligand and its metal complexes were tested on A-549, MDA-MB 231 and HEK293 cell lines. All compounds exhibit good potent cytotoxic agents that might become potent anticancer agent in clinical research.

Acknowledgment

We express our sincere thanks to the Chairman, Department of Industrial Chemistry, and Kuvempu University for providing laboratory facilities. Authors are also grateful to IISC Banglore, MIT Manipal, STIC Cochin and SAIF IIT Bombay for providing spectral data. We are thankful to the SDM Centre for Research in Ayurveda and Allied Sciences, Udupi for providing anticancer activity and Biogenic Hubli for providing DNA cleavage studies.

References

1. C. Rajarajeswari, R. Loganathan, M. Palaniandavar, E. Suresh, A. Riyasdeen, M. A. Akbarsha, Dalton Trans 42 (2013) 8347-8363.
2. Cancer Facts & Figures 2015, Atlanta, American Cancer Society, (2015).
3. T. C. Johnstone, K. Suntharalingam, S. J. Lippard, Chem. Rev.116 (2016) 3436-3486.
4. S. Banerjee, A.R. Chakravarty, Acc. Chem. Res. 48 (2015) 2075–2083.
5. B. Rosenberg, L.V. Camp, T. Krigas, Nature 205 (1965) 698–699.
6. G. Barone, A. Terenzi, A. Lauria, A. M. Almerico, J. M. Leal, N. Busto, B. García, C. Chem. Rev 257 (2013) 2848-2862.
7. VM. Manikandamathavan, T. Weyhermüller, RP. Parameswari, M. Sathishkumar, V. Subramanian, Nair BU. Dalton Trans. 43 (2014) 13018-13031.
8. R. Palchaudhri, P.J. Hergenrother. Curr. Opin. Biotechnol. 18 (2007) 497–503.
9. H. Abd El-Wahab, M Abd El-Fattah, A.H Ahmed, A.A Elhenawy, N.A Alian, Journal of Organometallic Chemistry (2015), doi: 10.1016/j.jorganchem.2015.05.024.
10. Yunpeng Du, Wei Chen, Xiang Fu, Hang Deng, JunGang Deng. RSC Adv. 6 (2016) 109718-109725.

11. G.L. Backes, D.M. Neumann, B.S. Jursic. Bioorg. Med.Chem. 22 (2014) 4629-4636.
12. R.N. Singh, Amit Kumar, R.K. Tiwari, Poonam Rawat, Divya Verma, Vikas Baboo. J. Mol. Struct. 1016 (2012) 97-108.
13. Nives Galic, Zvjezdana Cimerman, Vladislav Tomisic. Spectrochim. Acta A 71 (2008) 1274–1280.
14. Prateek Tyagi, Monika Tyagi, Swati Agrawal, Sulekh Chandra, Himanshu Ojha, Mallika Pathak. Spectrochim. Acta A 171 (2017) 246–257.
15. L.H. Abdel-Rahman, A.M. Abu-Dief, R.M. El-Khatib, S.M. Abdel-Fatah, J. Photochem. Photobiol. B 162 (2016) 298–308.
16. S. Budagumpi, N. V. Kulkarni, G. S. Kurdekar, M. P. Sathisha, V. K. Revankar, European J. Med. Chem., 45 (2010) 455-462.
17. S. Daravath, M.P. Kumar, A. Rambabu, N. Vamsikrishna, G. Nirmala, Shivaraj. J. Mol. Struct. 1144 (2017) 147-158.
18. P.R. Reddy, A. Shilpa, N. Raju, P. Raghavaiah, J. Inorg. Biochem. 105 (2011) 1603.
19. Hamid Khanmohammadi, Malihe Erfantalab, Spectrochim. Acta Part A 86 (2012) 39–43.
20. B. Sreekanth, G. Krishnamurthy, H. S. Bhojya Naik, T. K.Vishnuvardhan, Nucleosides, Nucleotides and Nucleic Acids. 31 (2012) 1-13.
21. S. Dhar, D. Senapati, P.K. Das, P. Chattopadhyay, M. Nethaji, A.R. Chakravarty, J. Am. Chem. Soc. 125 (2003) 12118–12124.
22. T.R. Mosmann, J. Immunol. Methods 65 (1983) 55-63.
23. S. K. N, G. Krishnamurthy, Y. D. Bodke, V. H. Malojirao, R. N. TR, S. Kandagalla and P. B T, *New J. Chem.*, 2018, DOI: 10.1039/C8NJ03057J.
24. W.J. Geary, Coord. Chem. Rev. 7 (1971) 81.
25. Abdel-Nasser M.A. Alaghaz , Mohamed E. Zayed, Suliman A. Alharbi, Reda A.A. Ammar, Ahmed Elhenawy. J. Mol. Struct. 1084 (2015) 352–367.
26. Gokhan Yeginer, Mehmet Gulcan, Sema Isik, Gulsiye Ozturk Urut, Sadin Ozdemir Mukerrem Kurtoglu. J Fluoresc 27 (2017) 2239–2251.
27. Ganga naik Krishnamurthy and Narashimaiah Shashikala. J. Serb. Chem. Soc. 74 (10) 1085–1096 (2009).
28. Munire Sarigul, Aysel Sari, Muhammet Kose, Vickie McKee, Mahfuz Elmastas, Ibrahim Demirtas,Mukerrem Kurtoglu. Inorganica Chimica Acta 444 (2016) 166–175.

29. A.Z. El-Sonbati, M.A. Diab, A.A. El-Bindary, M.I. Abou-Dobara, H.A. Seyam Journal of Molecular Liquids 218 (2016) 434–456.
30. A.M.A. Alaghaz, B.A. El-Sayed, A.A. El-Henawy, R.A.A. Ammar, Mol. Struct. 1035 (2013) 83–93.
31. Sirin Bitmez , Koray Sayin, Baris Avar, Muhammet Kose, Ahmet Kayraldız, Mukerrem Kurtoglu. J. Mol. Struct. 1076 (2014) 213–226
32. Nakamoto K (1997) Infrared and Raman spectra of inorganic and coordination compounds. Wiley, New York.
33. S.M. Pradeepa, H.S. Bhojya Naik, B. Vinay Kumar, K. Indira Priyadarsini, Atanu Barik, M.C. Prabhakara. Spectrochim. Acta Part A 141 (2015) 34–42.
34. E. Ispir, Dyes Pigments 82 (2009) 13–19.
35. Lever ABP (1984) Inorganic electronic spectroscopy. Elsevier, Amsterdam
36. T. Manjuraj, G. Krishnamurthy, Yadav D. Bodke, H.S. Bhojya Naik, H.S. Anil Kumar. J. Mol. Struct. 1171 (2018) 481-487.
37. D. N Sathyanarayana, electronic absorption spectroscopy and related technique University Press (India), Hyderabad 2001.
38. P.P. Dholakiya, M.N. Patel, Syn. React. Inorg. Met. Org. Nano-Met. Chem. 32 (2002) 819–829.
39. Mohamed Gaber, Yusif S. El-Sayed, Kamal El-Baradie, M. Rowaida, Fahmy. J. Mol. Struct. 1032 (2013) 185–194.
40. A.M.F. Benial, V. Ramakrishnan, R. Murugesan, Spectrochim. Acta Part A. 56 (2000) 2775–2781.
41. B. J. Hathaway and D. E. Billing. Coordin. Chem. Rev, 5 (1970) 143-207
42. Sreenu Daravath, Marri Pradeep Kumar, Aveli Rambabu, Narendrula Vamsikrishna, Nirmala Ganji, Shivaraj. J. Mol. Struct. 1144 (2017) 147-158.
43. P.R. Reddy, S. Rajeshwar, B. Satyanarayana, J. Photochem. Photobiol. B 160 (2016) 217–224.
44. Nirmala Ganji, Vijay Kumar Chityala, Pradeep Kumar Marri, Rambabu Aveli, Vamsikrishna Narendrula, Sreenu Daravath, Shivaraj, J. Photochem. Photobiol. B. 175 (2017) 132–140.
45. N. Divya Hegde, S. Ganesh Naik, Ramesh Vadavi, V. Shyam Kumar, A. Delicia Barretto, B. Kalagouda Gudasi. Inorganica Chimica Acta 461 (2017) 301–315.
46. D.J. Che, G. Li, X.L. Yao, Y. Zhu, D.P. Zhou, J. Chem. Soc., Dalton Trans. (1999) 2683–2687.

Manuscript Id: Our reference: MOLSTR 26394
Article reference: MOLSTR_MOLSTRUC-D-19-00214
Title **:** "Novel bioactive azo-azomethine based Cu (II), Co (II) and Ni(II) complexes, structural determination and biological activity"

As requested by the respective editorial team, the following corrections have been made and i request you to incorporate the changes given below. The corrections made were highlighted by the red colour font.

Table 4: Thermal decomposition of metal complexes.

Complex	Stage	Decomposition temp (^{0}C)	Probable assignment	Loss of mass in (%)		Residual species
				Obsd	Cald	
Cu[$C_{40}H_{38}N_{10}O_9$]	1st	30–78 °C	$3H_2O$	6.06	6.23	
	2nd	79–250 °C	C_4O_2	9.18	9.30	
	3rd	251–370 °C	$C_{10}H_{10}N_2$	17.96	18.26	CuO+2corbon
	4th	371-697 °C	$C_{24}H_{28}N_8O_3$	54.72	55.02	
	1st	26–75 °C	$2H_2O$	4.26	4.35	
Co[$C_{40}H_{36}N_{10}O_8$]	2nd	75–315 °C	$C_{12}H_{10}O_2N_2$	24.29	24.48	CoO
	3rd	315–495°C	$C_{28}H_{24}N_8O_3$	55.88	56.46	
	1st	28-65 °C	$2H_2O$	4.25	4.46	
	2nd	65-175 °C	$C_8H_4N_2$	15.56	15.71	
Ni[$C_{40}H_{36}N_{10}O_8$]	3rd	175-378 °C	$C_4H_2N_2O_2$	13.46	13.03	NiO
	4th	378-510 °C	$C_{28}H_{28}N_8O_3$	57.10	58.29	

Table 5: Powder X-ray data of Cu (II) complex.

Peak	2θ	θ	sinθ	$\sin^2\theta$	1000 $\sin^2\theta$	$h^2+k^2+l^2$	hkl	d		a in Å
								obs	calc	
1	10.98	5.49	0.0956	0.0091	9.153	1(1)	1 0 0	8.0575	8.387	8.052
2	17.05	8.50	0.1478	0.0218	21.86	2.3882(2)	1 1 0	5.2117	5.199	8.061
3	18.28	9.14	0.1588	0.0252	25.23	2.7564(3)	1 1 1	4.8507	4.834	8.099
4	22.48	11.24	0.1949	0.0379	37.99	4.1505(4)	2 0 0	3.9521	3.922	8.089
5	26.49	13.24	0.229	0.0524	52.49	5.7347(6)	2 1 1	3.3637	3.352	8.057
6	34.91	17.45	0.229	0.0899	89.97	9.8295(10)	3 1 0	2.5762	2.564	8.053
7	43.77	21.88	0.372	0.1389	138.93	15.178(15)	-	2.0706	1.988	8.048

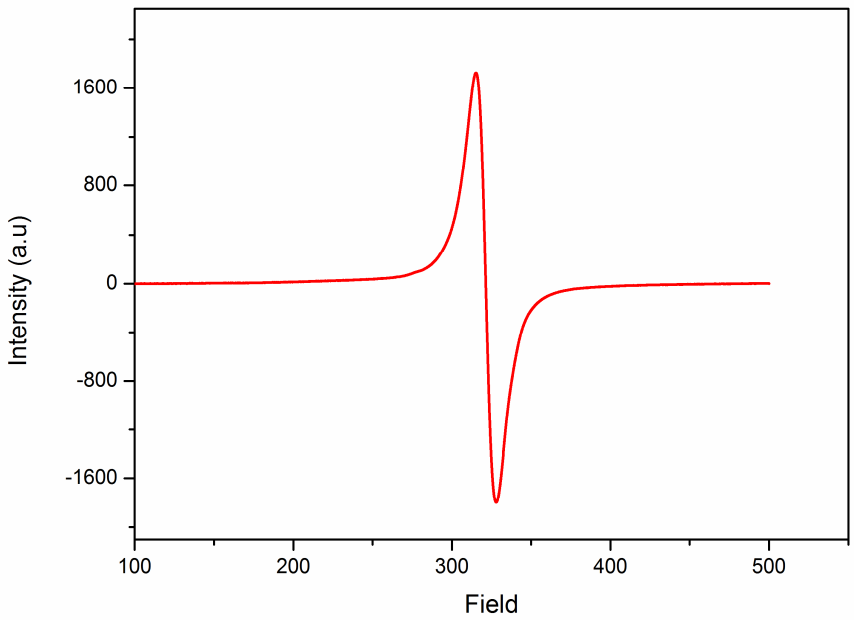

Fig. 1 ESR spectrum of complex **1a**

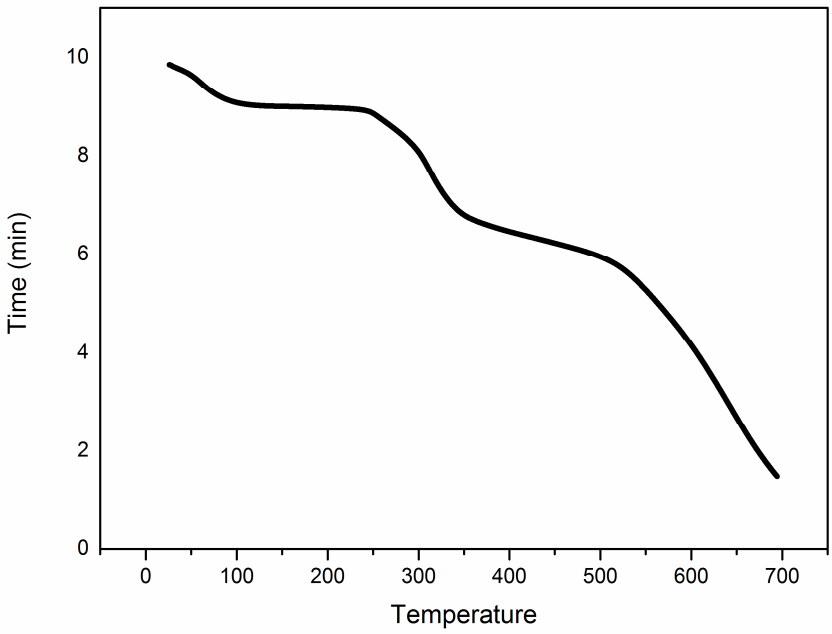

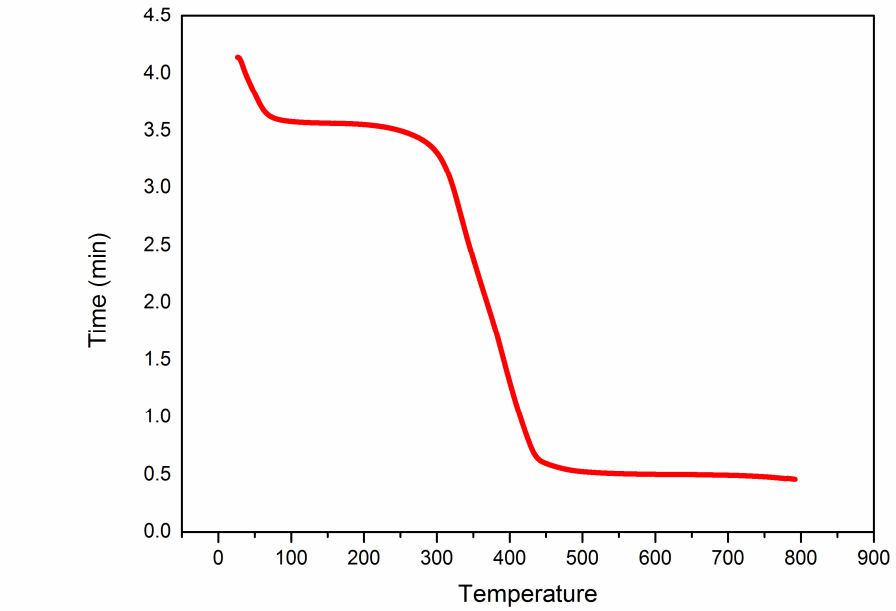

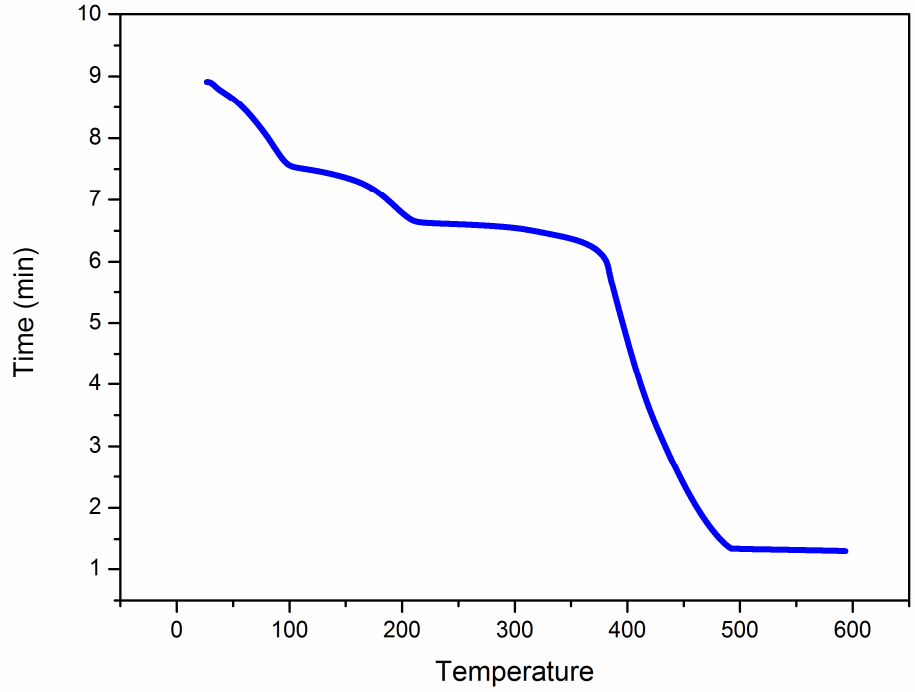

Fig. 2 TG curves of metal complexes (**1a-1c**)

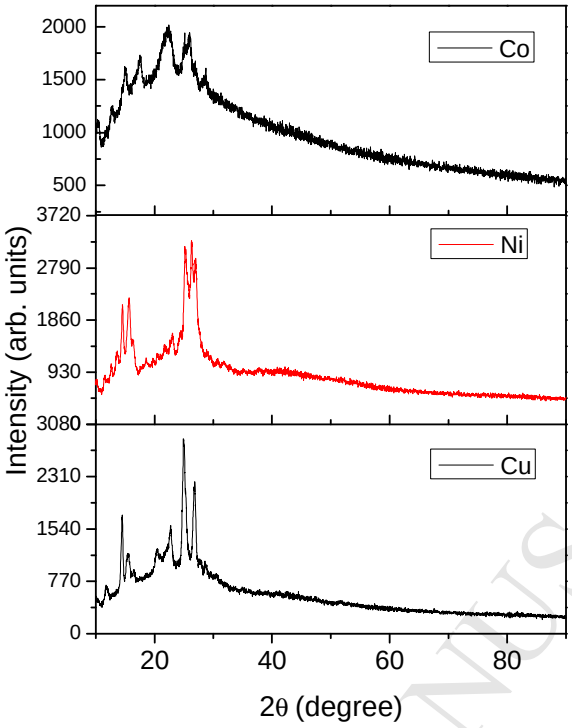

Fig. 3 Powder X-ray diffraction pattern of metal complexes (**1a-1c**)

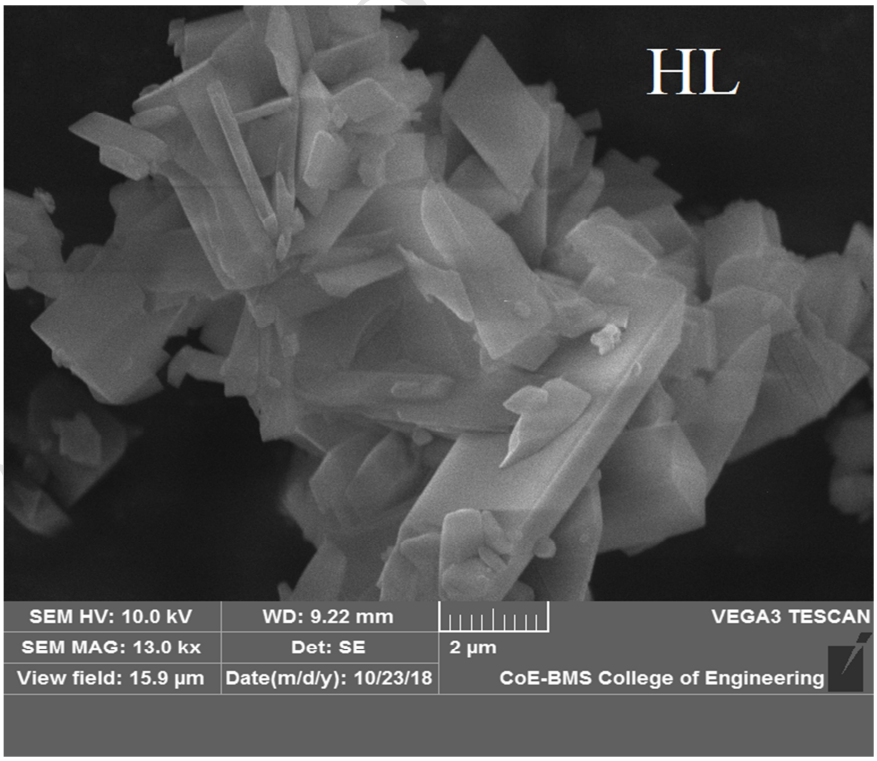

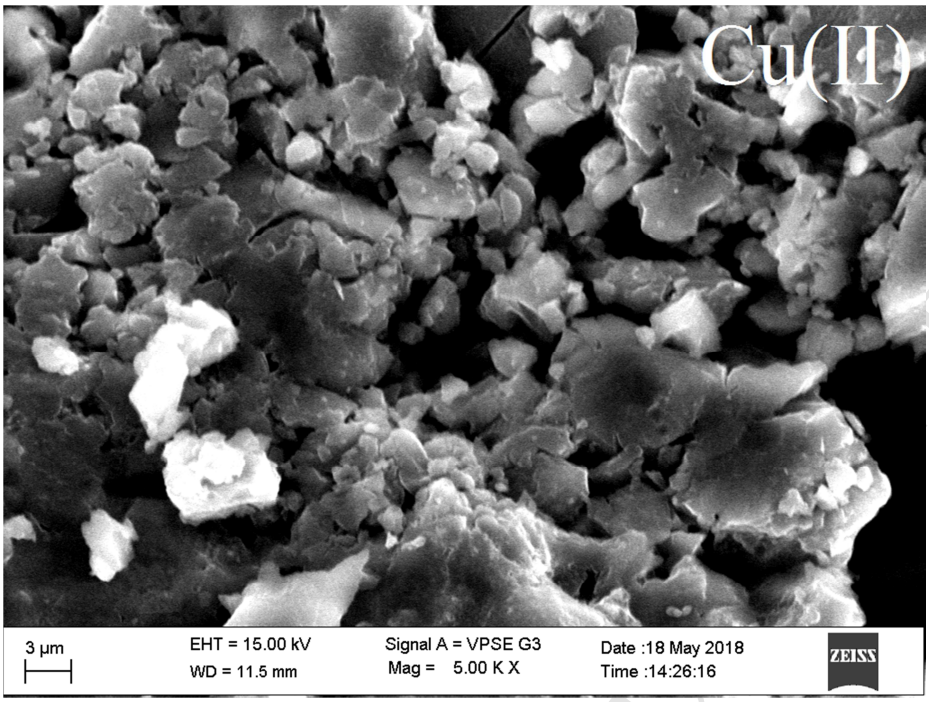
Cu(II)
3 µm
EHT = 15.00 kV
WD = 11.5 mm
Signal A = VPSE G3
Mag = 5.00 K X
Date :18 May 2018
Time :14:26:16
ZEISS

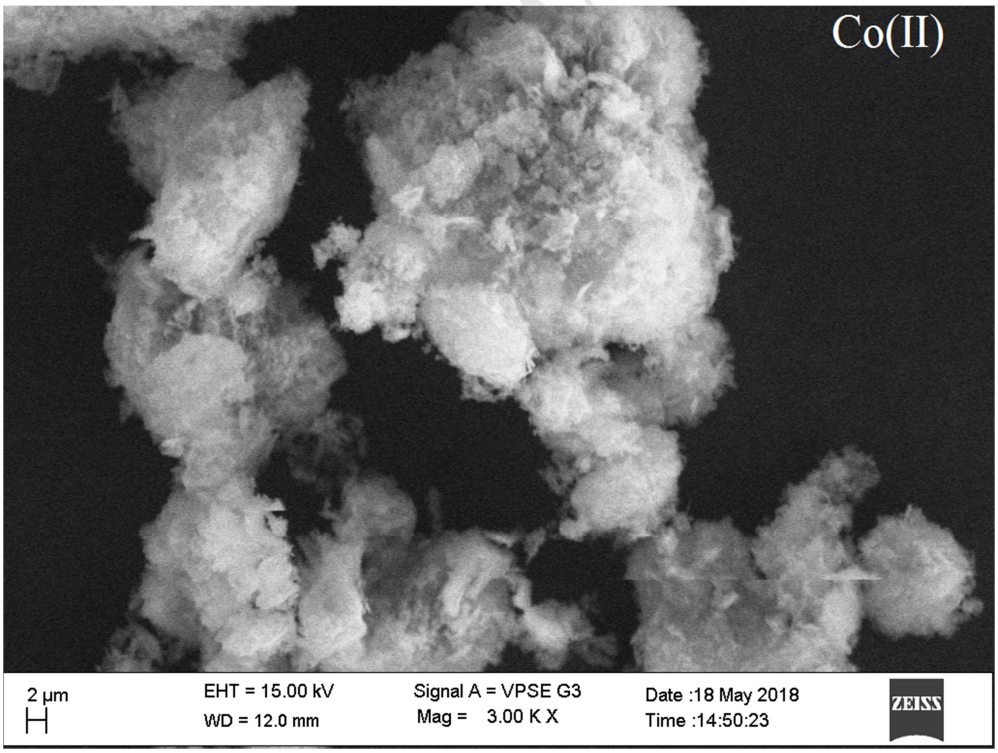
Co(II)
2 µm
EHT = 15.00 kV
WD = 12.0 mm
Signal A = VPSE G3
Mag = 3.00 K X
Date :18 May 2018
Time :14:50:23
ZEISS

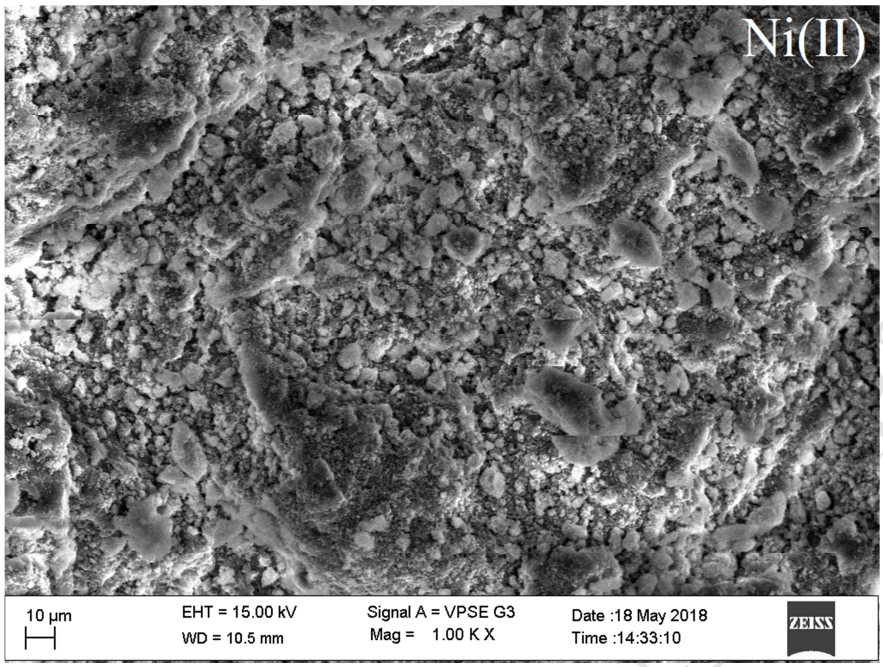

Fig.4 SEM images of ligands and its metal complexes

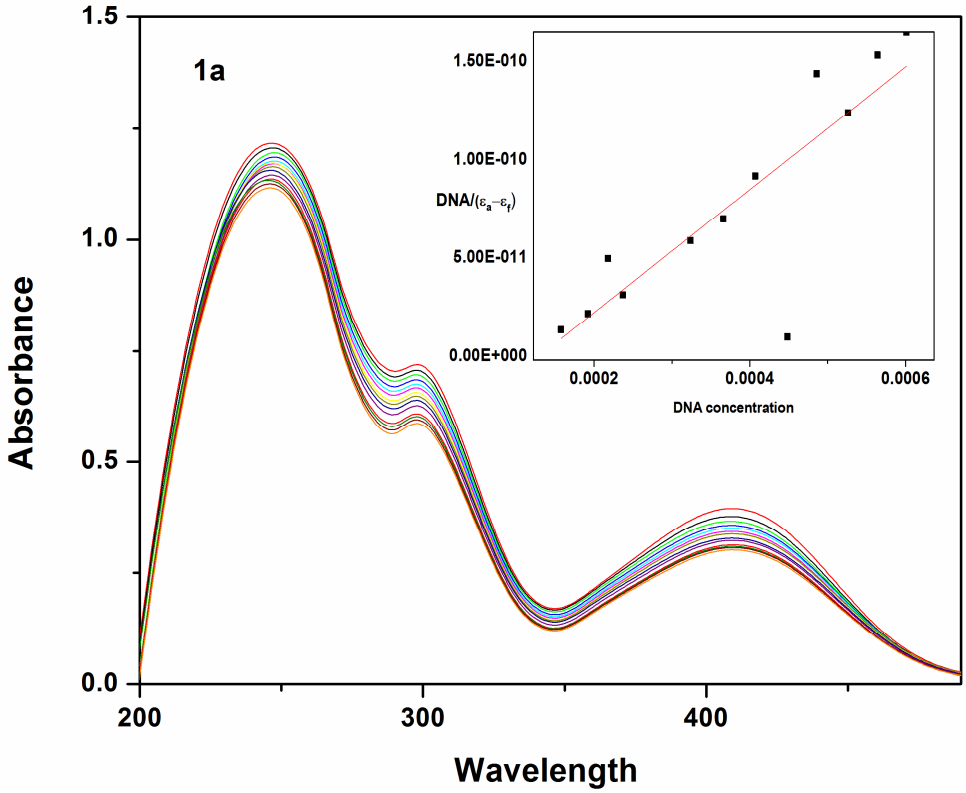

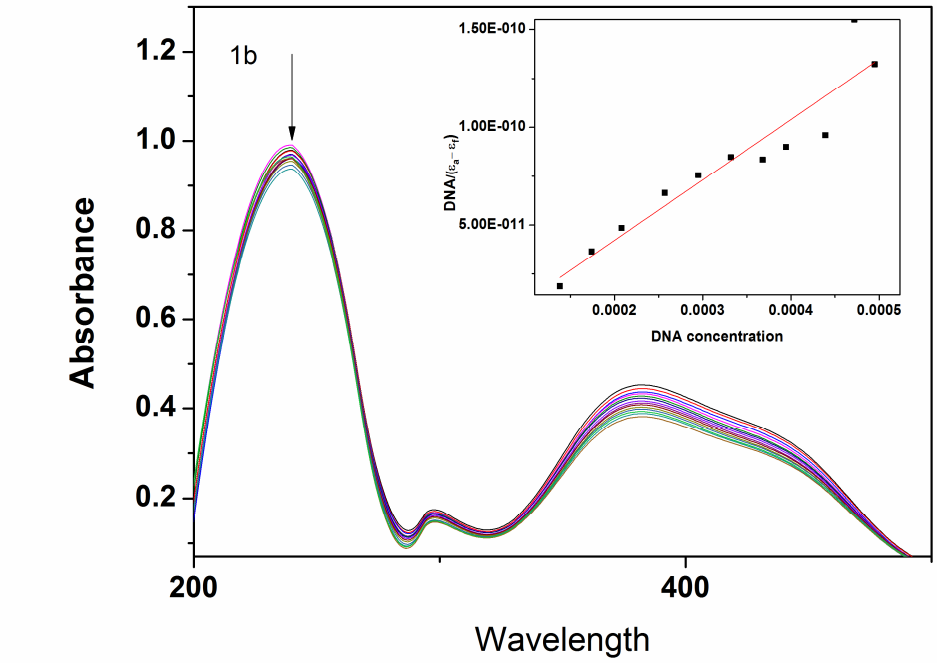

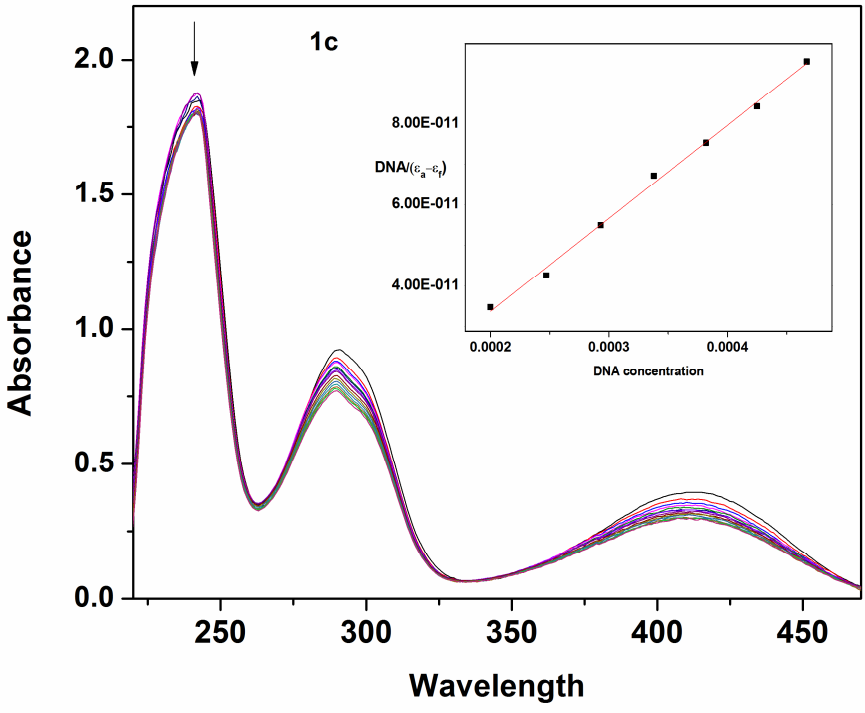

Fig.5 Electronic spectra of the complexes in Tris-HCl buffer upon addition of CT-DNA. Arrow shows the absorption intensities decrease in complex (**1a-1c**).

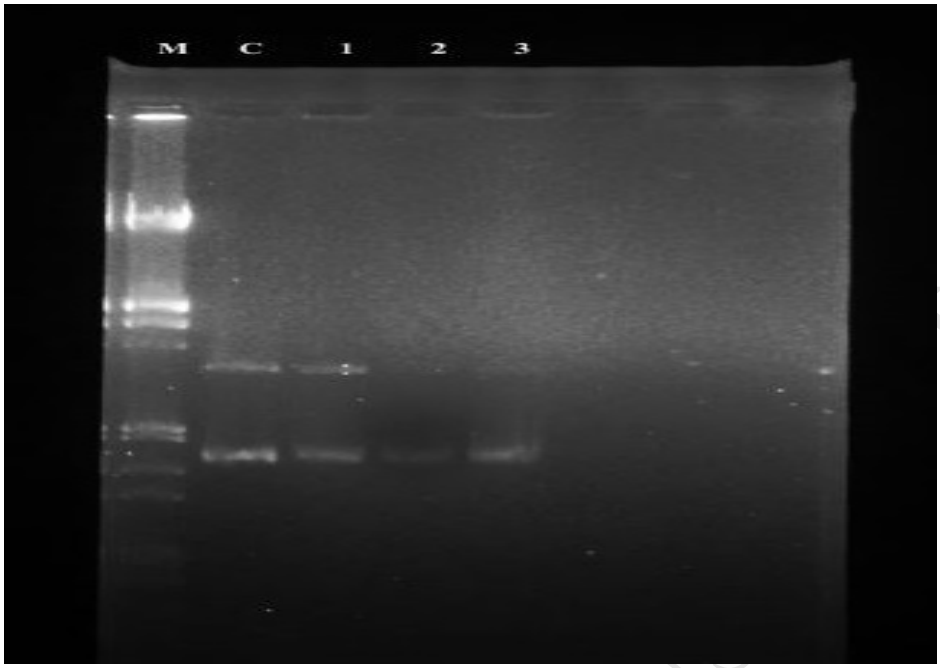

Fig. 6 Cleavage of supercoiled pBR322 DNA (2 µL, 2µg) at 37 ^{0}C in 5 mM Tris HCl/5 mM NaCl buffer by the metal complexes, M:. Marker, Lane 1: DNA control (pBR322), lane 2: DNA+1a complex, lane 3: DNA+1b complex, lane 4: DNA+1c complex.

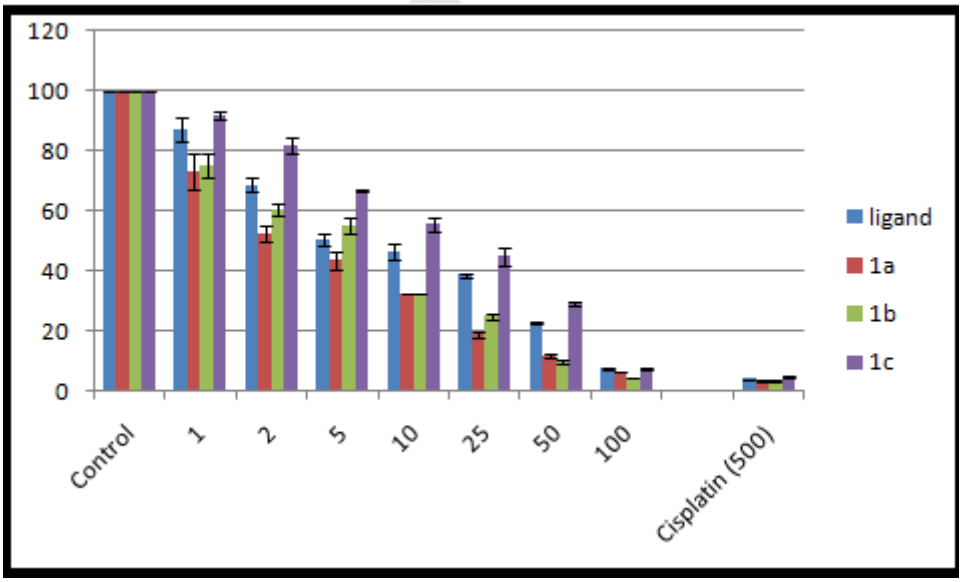

Fig. 7 Cytotoxicity effect of ligand and its complexes (**1a-2c)** on A549 cells assessed by MTT assay

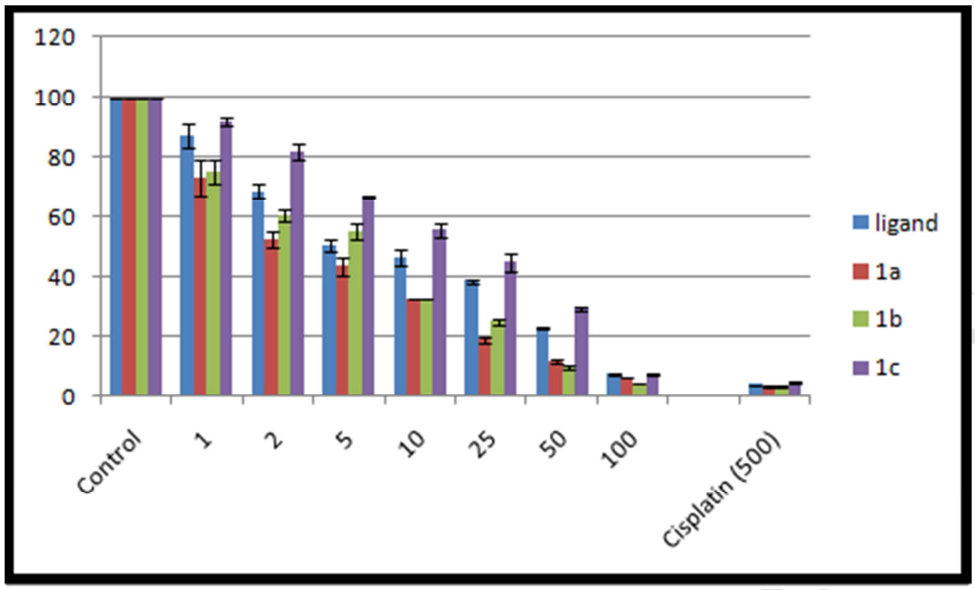

Fig. 8 Cytotoxicity effect of ligand and its complexes on MDA-MB-231 cells assessed by MTT assay

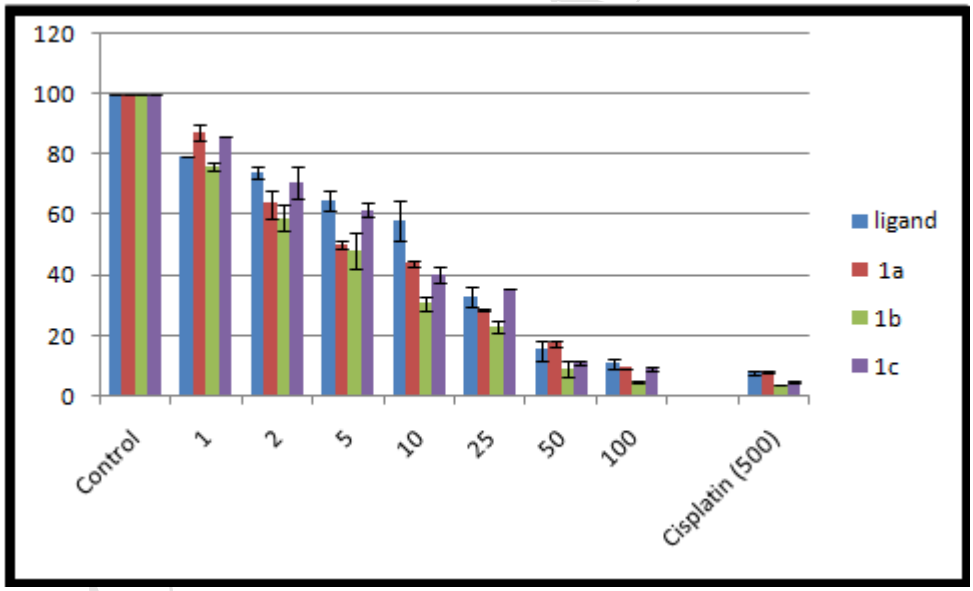

Fig. 9 Cytotoxicity effect of ligand and its complexes on normal Hek-293 cells assessed by MTT assay.

Highlights

- Synthesis and characterization of novel azo-azomethine ligand and its metal complexes.
- The ESR spectra of Cu (II) complexes confirm an octahedral geometry.
- Metal complexes act as good DNA intercalating agents and also cleave DNA efficiently.
- All metal complexes have showed good cytotoxic activity towards tested cell lines.